

# Measurement of Human Brain Lithium In Vivo by MR Spectroscopy

R. Gilberto González,<sup>1,2</sup> Alexander R. Guimaraes,<sup>2,4</sup> Gary S. Sachs,<sup>3</sup> Jerrold F. Rosenbaum,<sup>3</sup> Michael Garwood,<sup>5</sup> and Perry F. Renshaw<sup>2,3</sup>

**PURPOSE:** To quantify lithium in the human brain. **METHODS:** A <sup>7</sup>Li MR spectroscopy method was developed with special features for high precision including: a) sampling a large cerebral volume to maximize the signal-to-noise ratio; b) adiabatic excitation pulses to ensure uniform spin nutation; c) morphometric analysis of the MR images of the sampled cerebrum; d) a mathematical model derived from empirical data to correct for receiver inhomogeneity effects; and e) a long interpulse delay to eliminate errors arising from uncertain T1 values. **RESULTS:** A theoretical precision of 5.2% and an accuracy of better than 7.2% in someone with a brain lithium level of 1.0 mEq per liter of cerebral volume and precision and accuracy of 6.8 and 8.6%, respectively, in someone with 0.5 mEq/L brain lithium was calculated. This level of precision was surpassed in phantoms and patients. Brain lithium in 10 patients treated with lithium carbonate varied from 0.52 to 0.87 mEq/L (mean = 0.58 mEq/L; SD = 0.17 mEq/L). Brain-to-serum lithium ratios varied from 0.50 to 0.97 mEq/L (mean = 0.77 mEq/L; SD = 0.14 mEq/L). Substantial variation in brain lithium was observed in patients with similar serum lithium. **CONCLUSIONS:** A highly reliable method to quantify human brain lithium by <sup>7</sup>Li MR spectroscopy has been implemented. Unexpected variability in brain versus serum levels of lithium was detected in patients with bipolar disease.

**Index terms:** Drugs, psychoactive; Magnetic resonance, spectroscopy; Magnetic resonance, experimental; Brain, measurements; Brain, magnetic resonance

AJNR 14:1027-1037, Sep/Oct 1993

Lithium magnetic resonance spectroscopy (<sup>7</sup>Li MRS) is ideally suited for the direct study of the biodistribution and pharmacokinetics of lithium in people because of the unique ability of MR spectroscopy to measure directly and noninvasively the drug level in tissues. Many important questions regarding the use of lithium in the

treatment of patients with bipolar illness may be clarified by measuring the ion in its target organ, the brain. Although the utility of any method used in pharmacologic studies depends on its precision (reproducibility), accuracy, and practicality, the approaches published to date for determining brain lithium by <sup>7</sup>Li MRS have been of uncertain reliability and accuracy. This reflects the fact that true, quantitative <sup>7</sup>Li MRS is beset by a host of difficulties that are not easily overcome, most of which are also common to quantitative analysis by MRS of other nuclei, such as <sup>31</sup>P. The problems include low spin densities resulting in poor signal-to-noise ratios, uncertain T1 and T2 relaxation times, and inhomogeneous radio frequency excitation and reception caused by imperfect radio frequency coil design. The need for spatial localization creates additional sources of error. Some MR spectroscopists essentially ignore many of these obstacles by relying on a semiquantitative approach, the measurement of ratios of different MR spectral resonances. Others estimate the magnitude of each

Received April 17, 1992; revision requested July 22, received October 6, and accepted October 21.

<sup>1</sup> The Division of Neuroradiology, Department of Radiology, Massachusetts General Hospital, Harvard Medical School, Fruit Street, Boston, MA 02114. Address reprint requests to R. Gilberto González, MD, PhD.

<sup>2</sup> The MGH-NMR Center, Department of Radiology, Massachusetts General Hospital, Harvard Medical School, Charlestown, MA 02129.

<sup>3</sup> The Psychopharmacology Unit, Department of Psychiatry, Massachusetts General Hospital, Harvard Medical School, Boston, MA 02114.

<sup>4</sup> The Radiological Sciences Program, Department of Nuclear Engineering, Massachusetts Institute of Technology, Cambridge, MA 02139.

<sup>5</sup> The Center for Magnetic Resonance Research, University of Minnesota Medical School, Minneapolis, MN 55455.

This study was supported in part by U.S. Public Health Service Grant AG10679 to RGG.

AJNR 14:1027-1037, Sep/Oct 1993 0195-6108/93/1405-1027

© American Society of Neuroradiology

source of error and make the appropriate corrections. Although these approaches may suffice in certain circumstances, a more rigorous quantitative methodology may be required in others. The latter is the case for the pharmacokinetic studies of lithium in the brain.

In this article, we describe a method, implemented in a clinical MR unit, that substantively overcomes the obstacles to quantitative analysis of brain lithium by MRS. Key components of the method include a large sample size to maximize the signal-to-noise ratio, adiabatic radio frequency pulses to minimize radio frequency transmitter inhomogeneity effects, morphometric analysis of proton MR images to measure accurately the brain volume sampled by MRS, an empirical model to correct for radiofrequency receiver inhomogeneity, and a long repetition time (TR). The error analysis included in this study provides guidelines on the concentrations of the ion in the human brain, which can be reliably monitored by  $^7\text{Li}$  MRS. The error analysis was verified by studies on phantoms and patients. A preliminary clinical study is also reported; the results suggest that direct brain lithium measurements will have important clinical implications.

## Materials and Methods

### *Instrumentation and Materials*

MR studies were performed on a commercial 1.5-T MR imager (GE Signa, Milwaukee, WI). For proton MR, the quadrature body coil was used.  $^7\text{Li}$  MRS studies were performed with an Alderman-Grant-type coil (1), which was constructed in-house, 24 cm in diameter, tuned to 24.8 MHz. The same external standard reference source was used for all phantom and human studies. The external standard is fixed on the inner margin of the lithium head coil and consists of a MR tube 10 mm in diameter, filled with a solution of  $\sim 0.5$  mol/L LiCl and 135 mmol/L  $\text{DyCl}_3$ . The dysprosium serves as a chemical shift reagent (the Li resonance is shifted approximately 15 ppm downfield) and as a relaxation agent to keep the external standard lithium T1 well below 5 seconds.

Phantom studies were performed with variable concentrations of lithium chloride (Sigma, St. Louis, MO) and 145 mmol/L NaCl dissolved in distilled water. These solutions also contained  $\sim 3$  mmol/L gadolinium-DTPA (Berlex Laboratories, Wayne, NJ) to reduce the lithium T1 to under 5 seconds. The solutions were contained in 2-L plastic cylinders, 10 cm in diameter. True phantom and serum lithium concentrations were determined by atomic absorption spectroscopy at the hospital clinical laboratories.

### *Proton MR Data Acquisition*

All studies on human subjects were approved by the hospital subcommittee on human studies. Patients typically undergo MR imaging and spectroscopy in the following manner: informed consent is obtained from each patient, and 5 mL of blood is drawn for serum lithium determination by atomic absorption spectroscopy. The subject is placed in the magnet with the  $^7\text{Li}$  radio frequency head coil appropriately positioned. Once the patient is in the magnet the head coil is tuned and matched. T1-weighted sagittal  $^1\text{H}$  MR images, 600/20 (TR/TE), are obtained with the body coil. The appropriate axial section for MRS is selected from the midline section of the sagittal image data set. The 6-cm MRS section is typically centered 1 cm superior to the body of the corpus callosum. The patient table is moved to center the selected section in the gradient isocenter of the magnet. T1-weighted axial  $^1\text{H}$  MR images (600/20, 4 excitations) are obtained from the selected section. Five sections 10 mm thick with a 2.5-mm gap, are acquired. The procedure up to this point takes 8 to 10 minutes. Shimming is then performed on the selected 6-cm section with the water resonance and the depth-resolved surface spectroscopy pulse sequence (2). It takes approximately 5 minutes to achieve a line width of 20 Hz or better.

### *Lithium MRS Data Acquisition*

After obtaining the proton MR data and shimming, the transmitter coaxial cables are removed from the 2 Signa PTS 100 frequency synthesizers and connected with a "T" coaxial connector to a single PTS 100 frequency synthesizer. The frequency is manually tuned to the  $^7\text{Li}$  Larmor frequency at 1.5 T ( $\sim 24.825$  MHz). This method is used because the Signa software does not support the lithium nucleus. The Signa transceiver frequency is set to the nearest allowed frequency, which is the Larmor frequency for  $^{31}\text{P}$  ( $\sim 25.8$  MHz). The adiabatic one-dimensional image-selected in vivo spectroscopy (1D-ISIS) pulse sequence (described below) is down-loaded and a  $^7\text{Li}$  MRS spectrum is then acquired from the selected 6-cm section with a TR of 25 seconds. 50 acquisitions are averaged, which takes less than 21 minutes. The spectral width is 1000 Hz, and 1024 points are sampled. MR and MRS data from the calibration phantoms are obtained at the end of the session with the same parameters, except that MRS data collected from the calibration standards are averaged for approximately 1 hour ( $\sim 150$  averages).

### *$^7\text{Li}$ MRS Pulse Sequence*

The lithium MRS pulse sequence is a modification of the 1D-ISIS method first proposed by Bottomley and Hardy (3) for human studies of phosphorus metabolites. The ISIS method was originally described by Ordidge et al (4). The pulse sequence is shown in Figure 1. It consists of an adiabatic, frequency-selective, 180-degree inversion pulse (5) (8-millisecond pulse width) executed in the presence of a linear gradient along the z direction, followed without

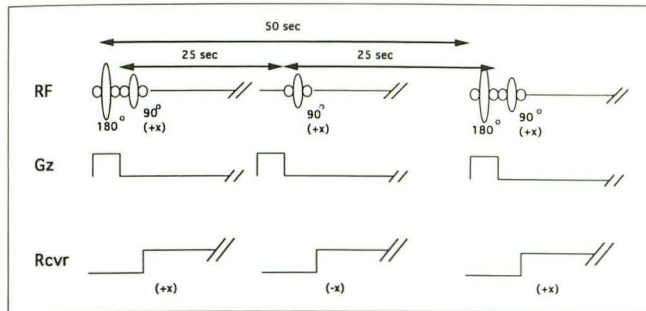


Fig. 1. Adiabatic 1D-ISIS pulse sequence.

This pulse sequence results in the collection of MR spectroscopic data from a well-defined axial section through the brain. The complete sequence is executed over two TR periods. During the initial TR period, the first radiofrequency pulse, an adiabatic, frequency-selective inversion pulse (Silver-Hoult), is applied in the presence of a magnetic field gradient along the subject's longitudinal axis ( $G_z$ ). This inverts the spins only within a well-defined axial section. Immediately after the inversion pulse, a nonselective, adiabatic, 90-degree pulse (BIR-4) is applied in the absence of a gradient that nutates all spins within the brain into the transverse plane. However, all spins within the selected axial section are oriented with a 180-degree phase shift ( $-x$ ) relative to the spins outside the section ( $+x$ ). The FID is collected in the averager with the receiver (Rcvr) phase in its usual value relative to the transmission radiofrequency ( $+x$ ). During the second TR period, the inversion pulse is not applied; only the nonselective, adiabatic, 90-degree pulse is applied across the whole sample. The receiver collects the FID immediately after the pulse but with the receiver phase shifted 180 degrees ( $-x$ ). Thus, the signal from spins within the selected section averages coherently, whereas all signals outside the section cancel.

delay by a nonselective, adiabatic 90-degree pulse (6) (4-millisecond pulse width) in the absence of a gradient. To ensure an adequate lithium signal-to-noise ratio, a section 6 cm thick is used. The signal, known as the free induction decay or FID, is collected immediately after the 90-degree pulse. Twenty-five seconds after the initial 90-degree pulse, another nonselective, adiabatic, 90-degree pulse is executed with the receiver phase shifted by 180 degrees, and the FID is added in the averager. By this method, the signals arising within the selected section will add coherently and all signals arising outside the section will cancel. The entire pulse sequence is repeated 50 seconds after the initial frequency-selective, 180-degree inversion pulse. In less than 21 minutes, 50 90-degree excitation pulses are averaged. Because the TR is more than five times the T1 of brain lithium ( $\sim 4.2$  seconds by our measurements and similar values found by others working at 2.0 T (7)), the resulting spectrum has a lithium resonance the area of which is directly proportional to the lithium concentration.

The method is quantitative if all nuclei within tissues and the calibration phantom experience the same spin nutation after each pulse. This is achieved in the presence of nonuniform B1 fields through the use of adiabatic pulses. A discussion of the principles of adiabatic pulses may be found in the article by Staewen et al (6).

### Proton MR Image Morphometric Analysis

Morphometric analysis of proton MR images is performed by the use of a semiautomated, computerized method based on high-resolution MR imaging data developed in-house. By this method, whole brain volumes, volumes of individual substructures, and lesion volumes can be derived. On each planar MR section, an intensity contour mapping algorithm creates continuous outlines based on the pixel signal intensity distribution. A sample of foreground and background straddling a border is selected by the investigator. The neighborhood of these points is analyzed by Fisher's discriminant method to determine a least-cost border that forms a continuous contour. To determine the volume of a given structure, the number of pixels contained within that structure is determined and is multiplied by the section thickness. Fuzzy edge classification is applied to correct for edge dichotomization, and a linear mixture model corrects partial volume effects. An example of a part of such an analysis is shown in Figure 2.

This method is applied to each of the five T1-weighted axial sections obtained from the selected 6-cm section used for lithium MRS data acquisition. Brain parenchyma, cerebrospinal fluid (CSF), and extracranial muscle volumes are determined separately. The brain parenchyma area for each section is multiplied by 12 mm, and the results from all five sections are summed to give the total brain volume sampled by  $^7\text{Li}$  MRS. By this method, it is possible to account for the volumes of the gaps by linear extrapolation



Fig. 2. Brain MR morphometric analysis.

An example from a part of the morphometric analysis procedure is displayed here. Typically, five axial T1-weighted images through the selected section are acquired. One image from such an image set is shown. A sample of foreground and background straddling a border was selected by the investigator. The neighborhood of these points was analyzed with the software by the use of Fisher discriminant method to determine a least-cost border that forms a continuous contour. The resultant contours are displayed on this image. The software provides the number of pixels within each contour and, if desired, the position and intensity of each pixel.

from the adjacent measured sections. A similar procedure is followed for muscle and CSF fluid volumes.

#### Lithium MRS Data Processing

$^7\text{Li}$  MRS data are analyzed on a Sun SPARCstation with NMR1 software (New Methods Research, Inc., East Syracuse, NY). The FID is first processed with an exponential filter, resulting in a line broadening of 10 Hz. The FID is then Fourier transformed and manually phased. The areas of the lithium resonances that arise from the brain (or phantom) and the external standard are determined by integration. The lithium concentration is calculated using equation 1 as described below. The concentration is expressed in milliequivalents per liter.

#### Brain Lithium Concentration Calculation

Determination of the brain lithium concentration by the method presented here requires  $^7\text{Li}$  MRS measurements of calibration phantoms with known concentrations of lithium. Such measurements are performed as closely as possible to the patient studies to minimize errors due to instrument instability. Usually, the calibration phantom studies were performed immediately after the last patient had  $^7\text{Li}$  MRS performed. Initially, calibration curves were drawn using data from three different calibration phantoms that contained different concentrations of lithium. Because these calibration curves were found to be highly linear, subsequent studies used a single calibration phantom. The spectrum from the calibration phantom is acquired with the same parameters as those used for human studies, with the exception that the phantom data are acquired for a longer period, about 1 hour, to improve the signal-to-noise ratio of the calibration phantom spectrum. The phantom consists of a known concentration of lithium chloride (~2 mmol/L independently determined by atomic absorption spectroscopy) in a 145 mmol/L NaCl solution contained within a 2-L plastic cylinder. The 2 mmol/L phantom concentration was chosen because, with a 6-cm section thickness, a volume of about 600 mL is sampled. Thus, the number of lithium spins excited is similar to the number of spins expected in the human brain.

The brain lithium concentration is calculated by use of the following formula:

$$[L] = \frac{S_b}{S_c} \times \frac{V_c}{V_b} \times L_c \times C_r \times C_{T1} \times C_{T2} - L_x \quad (1)$$

where [L] is the brain lithium concentration;  $S_b$  is the ratio of the brain lithium resonance area to the external standard resonance area;  $S_c$  is the ratio of the calibration phantom lithium resonance area to the external standard resonance area;  $V_c$  is the sampled volume of the phantom;  $V_b$  is the patient brain volume sampled;  $L_c$  is the concentration of lithium within the calibration phantom;  $C_r$  is a correction factor for radio frequency receiver inhomogeneity, which is described below;  $C_{T1}$  and  $C_{T2}$  correct for partial saturation effects and transverse relaxation time effects, respectively;

and  $L_x$  corrects for extracerebral contributions to the lithium signal primarily from muscle, CSF and blood.

#### Correction Factors

Because the TR is more than five times the T1 of lithium in the subjects and phantoms,  $C_{T1}$  is equal to one. The finite length of the excitation pulses will result in a slight loss of signal due to T2 decay. However, within the error of our method, the difference in relative signal loss between the subject and the phantom is not detectable. Thus,  $C_{T2}$  is also unity.

Radio frequency receiver inhomogeneity effects are compensated for through the use of an empirically derived correction factor,  $C_r$ . The radio frequency receiver inhomogeneity was mapped with measurements of a 1-mL sample of concentrated lithium chloride positioned in different locations within the coil. The coil was loaded to the same degree as a human head with normal saline solution in a flexible plastic bag. Excitation was achieved with the adiabatic 1D-ISIS sequence. Measurements revealed substantial variation in the signal amplitude as a function of sample position in the transverse plane. In general, the closer the sample was positioned to the coil, the higher the signal. However, the change in signal was nonlinear. Little variation in signal was detected by a change in position perpendicular to the transverse plane. Thus, the data were fit to a two-variable (ie, the transverse plane coordinates  $x$  and  $y$ ), eighth-power polynomial function by a least-squares algorithm. A plot of this function is shown in Figure 3.

The receiver inhomogeneity correction factor is determined in the following manner. As previously described, axial T1-weighted images are obtained from the same brain region that is sampled by  $^7\text{Li}$  MRS, and they are morphometrically analyzed. For each axial section, the coordinates of the brain parenchyma relative to the external standard are extracted. The sampled brain volume for each section is transformed into a collection of approximately 1000 to 1200 elements. An example of such a data set is shown in Figure 4. The assumption is made that the concentrations of lithium in all elements are equal. The expected receiver inhomogeneity deriving from each point in space is calculated by use of the empirically derived polynomial function described in the previous paragraph. The result from each point is summed, and the total is divided by the total number of points to give the average receiver inhomogeneity factor for the entire sampled volume. A similar procedure is then followed for the calibration phantom data. The ratio of the average receiver inhomogeneity factor for the brain to the average receiver inhomogeneity factor for the calibration phantom gives  $C_r$ .

Lithium signal extrinsic to the brain is assumed to arise predominantly from muscle and CSF. The muscle lithium contribution is calculated on the basis of the volume of muscle within the section of interest as measured by morphometric analysis, assuming a concentration three times the brain concentration (see reference 17). A similar procedure is followed for determining the contribution from the CSF lithium with the assumption that the CSF lithium

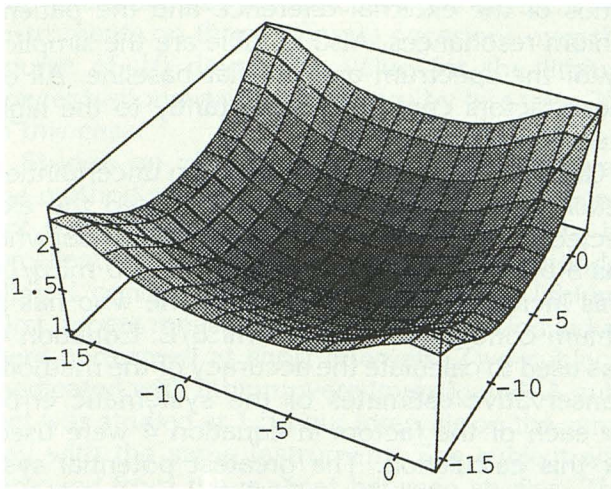


Fig. 3. Receiver inhomogeneity correction function.

This model was derived from empirical data obtained by positioning a small sample of concentrated LiCl in different positions within the coil and by collecting a spectrum at each location by adiabatic excitation. The integral of the Li resonance from each position reflects the receiver sensitivity of the coil to spins at that location. The three-dimensional data set (two spatial dimensions,  $x$  and  $y$ , and resonance integral) was fit to an eighth-power polynomial function by a least-squares algorithm of the Mathematica software (Wolfram Research, Inc., Champaign, IL). The same software was then used to plot the function that is shown here.

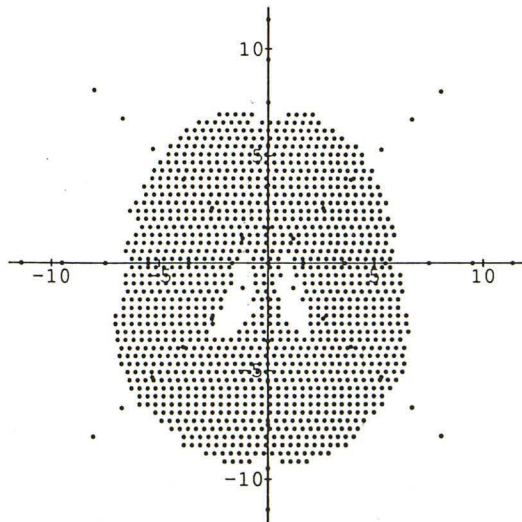


Fig. 4. Finite element plot of single axial brain section.

The coordinates of brain parenchyma relative to the external standard of each axial T1-weighted image are extracted and transformed into a collection of approximately 1000 to 1200 elements, as shown in this example. Each point in the resultant plot is then used for receiver inhomogeneity correction as described in the methods.

concentration is 0.35 times the serum concentration (see reference 28). The blood contribution is estimated from the serum concentration and assuming a cerebral blood volume of 5% of the brain volume. The sum of these contributions is then subtracted from the total measured lithium. The brain lithium concentration is expressed in milliequivalents per liter of brain tissue.

Corrections for brain motion and blood flow effects were not applied. The brain lithium signal is averaged over 21 minutes with sampling at 25-second intervals. Thus, the signal arises from a time-averaged volume. The images that are used to determine the volume estimate are also averaged over several minutes. It is assumed that this average volume is the same as in the lithium measurement; therefore, motion effects are properly compensated. Blood flow effects are expected to be miniscule because the signal is acquired immediately after the 90-degree pulse and all spins that are in the excited section will provide signal even if they move out of the section when the signal is being collected.

#### Error Analysis

The expected precision of the method can be calculated by use of the following equation:

$$\frac{\sigma^2(L)}{L^2} \cong \frac{\sigma^2(S_b)}{S_b^2} + \frac{\sigma^2(S_c)}{S_c^2} + \frac{\sigma^2(V_b)}{V_b^2} + \frac{\sigma^2(V_c)}{V_c^2} + \frac{\sigma^2(L_c)}{L_c^2} + \sigma^2(L_x) \quad (2)$$

where  $\sigma(L)$  is the random error for the brain lithium concentration due to random error contributions from each of the factors used for its calculation. The other factors in equation (2) are as defined for equation (1). The random uncertainties for most of the factors were estimated with empirical data. The uncertainty in the ratio of the brain lithium resonance to the external standard resonance,  $\sigma(S_b)$ , was estimated with the root-mean-square signal-to-noise values for each resonance with the NMR1 spectral analysis software. The uncertainty for the calibration phantom lithium-to-external standard resonance ratio,  $\sigma(S_c)$ , was also determined in this manner. Typical signal-to-noise ratios varied from 20:1 to 30:1 for the brain lithium resonance and 70:1 for the external standard resonance. The uncertainty of the measured brain volume is estimated to be on the order of 3% on the basis of experimental studies on phantoms. The calibration phantom volume random uncertainty is very low, <1%, because of its uniform, well-defined geometry. The random uncertainty in the calibration phantom lithium concentration is the uncertainty inherent in the atomic absorption method and was found to be about 2.9% for 2 mEq/L samples. The reproducibility of the calculation for the receiver inhomogeneity correction factor was found to be very high, with less than 1% variation. The random error contribution from CSF, blood, and muscle lithium was estimated to be proportional to the overall random error (ie ~5% to 7%).

The accuracy (uncertainty due to systematic error) of the method can be estimated by the use of the following equation:

$$\Delta L \cong \frac{\partial L}{\partial S_b} \Delta S_b + \frac{\partial L}{\partial S_c} \Delta S_c + \frac{\partial L}{\partial V_c} \Delta V_c + \frac{\partial L}{\partial V_b} \Delta V_b \quad (3)$$

$$+ \frac{\partial L}{\partial L_c} \Delta L_c + \frac{\partial L}{\partial C_r} \Delta C_r + \frac{\partial L}{\partial C_{T1}} \Delta C_{T1}$$

$$+ \frac{\partial L}{\partial C_{T2}} \Delta C_{T2} + \frac{\partial L}{\partial L_x} \Delta L_x$$

where the accuracy of the brain lithium concentration ( $\Delta L$ ) is equal to the sum of the partial derivative of equation (1) with respect to each factor times the systematic error of each factor. For most of the factors, only random errors are expected and, therefore, do not contribute to systematic uncertainty (eg,  $\Delta S_b = 0$ , etc). Systematic errors are expected from the receiver inhomogeneity correction factor and in the contribution of lithium signal from extracerebral sources, mostly muscle, blood, and CSF. Thus, equation (3) reduces to the following:

$$\Delta L \cong \frac{\partial L}{\partial C_r} \Delta C_r + \frac{\partial L}{\partial L_x} \Delta L_x \quad (4)$$

## Results

A typical lithium MR spectrum from the brain of a patient is shown in Figure 5. This patient was medicated with a daily oral dosage of 1575 mg of lithium carbonate. The brain lithium concentration was calculated to be 0.85 mEq/L. Particular note is made of the high signal-to-noise

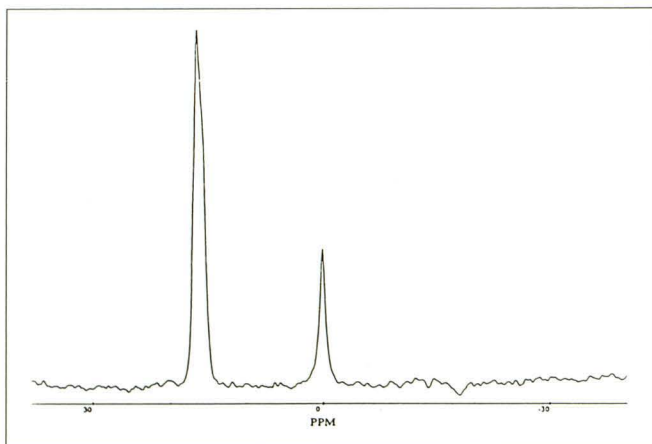


Fig. 5. In vivo human brain  $^7\text{Li}$  MR spectrum.

This spectrum was acquired from a 6-cm axial section through the brain of patient orally taking 1.6 g of lithium carbonate each day. MR spectral parameters are delineated in the methods. The resonance on the left arises from the external standard. The resonance on the right arises from lithium within the patient. The majority of the signal is from the brain with small contributions from muscle, CSF, and blood.

ratios of the external reference and the patient lithium resonances. Also notable are the simplicity of the spectrum and the flat baseline. All of these factors contribute importantly to the high precision of the method.

Using equation 2 and the random uncertainties detailed in the methods, we calculated the expected precision to be 5.2% for an individual who has a brain lithium concentration of 1.0 mEq/L. This increases to 6.8% for someone who has a lithium concentration of 0.5 mEq/L. Equation 4 was used to calculate the accuracy of the method. Conservative estimates of the systematic error for each of the factors in equation 4 were used for this calculation. The greatest potential systematic error arises from  $C_r$ , the correction factor for receiver inhomogeneity. A somewhat extreme example was used to estimate the upper limit of  $\Delta C_r$ : if all of the brain lithium was concentrated in a central cylindrical volume of 500 mL within the brain, instead of being evenly distributed throughout the  $\sim 1000$ -mL volume sampled, then this would result in the  $C_r$  value being about 0.1 units higher than its usual value of about 0.9. This would contribute to a systematic error of 5.7% in a person with a 1 mEq/L brain lithium concentration. This can be considered to be the upper limit of the systematic error from this source. For  $\Delta L_x$ , we may conservatively estimate that each of the contributors (ie, muscle, blood, and CSF) to this error factor may be erroneous by 30%. Together, they would propagate to add a total error of 1.5%. A very conservative estimate for the accuracy of the method is therefore  $<7.2\%$ . A similar analysis performed with an assumed brain lithium concentration of 0.5 mEq/L resulted in an estimated accuracy of  $<8.6\%$ .

In summary, the calculation of the theoretical random and systematic errors in the determination of the brain lithium concentration by the method described results in an estimated precision of 5.2% and an accuracy of  $<7.2\%$  for a person whose brain lithium concentration is 1.0 mEq/L and a precision of 6.8% and an accuracy of  $<8.6\%$  for a person whose brain lithium concentration is 0.5 mEq/L.

The reliability of the lithium MRS method was evaluated in phantoms and in patients. The goal was to verify the estimated precision. The first series of studies involved repeated measures of phantoms that had LiCl concentrations of 1 and 2 mmol/L. Under these conditions, the measured lithium concentration varied by less than 2%. One phantom containing a 2 mmol/L concentra-

tion of lithium was measured by two different MR instruments on three separate occasions over the course of 10 days. The value for the lithium concentration was found to vary by less than 3% in this case.

Studies on phantoms provide information on the method's precision under optimal conditions; not surprisingly, the precision was found to be excellent. The method was next evaluated under clinical conditions in individuals taking lithium. First, repeat measurements in the same individual were performed at short intervals. Two subjects medicated with lithium were investigated. A subject was studied at 1.5-hour intervals on the same day with the same instrument. The subject was removed from the magnet between studies. The results of this study are shown in Table 1 (see subjects A and B). The reproducibility of the method in this study proved to be excellent; it was in fact better than the calculated, theoretical precision. The variations in measured brain lithium were 2.9% for subject A and 2.3% for subject B. Of particular note, Table 1 reveals that, for each of these two subjects, the amount of brain sampled was very similar in both studies: variations of brain volumes measured 1.8 and 3.0% for subjects A and B, respectively. This indicates high reproducibility in patient positioning and spatial localization for spectral acquisition, a factor that becomes very important in serial pharmacokinetic studies.

A second study was undertaken in an attempt to assess the method's precision over a substantially longer interval. A patient medicated with lithium was studied twice over a 6-month interval. The subject was selected because he was considered reliable and clinically stable and had been

on the same dosage of lithium carbonate for several months before the study. He remained clinically stable and continued to receive the same dosage of lithium throughout the duration of the study. The amount of brain sampled was different in each study: a section 4 cm thick was first selected, and a section 6 cm thick was studied on the second examination. The discrepancy in the section thicknesses was the result of our efforts to determine optimal section thickness; this patient was one of the first studied. The results are shown in Table 1 as subject C. The measured brain lithium concentration varied little, 0.89 mmol/L on the first examination and 0.87 mmol/L on the second. Although it is impossible to verify the true variation in brain lithium in this patient at these two times the clinical stability, nonchanging lithium dosage, and the patient's history of reliability would suggest the establishment of a steady-state brain lithium concentration. The data strongly suggest that the proposed method is highly reproducible over periods of at least 6 months.

Having confirmed the precision of the method in phantoms and patients, a pilot clinical study was undertaken. Ten patients who were on daily dosages of lithium carbonate of 900 mg/d up to 1575 mg/d were studied. The mean daily dosage was 1328 mg. Before each MRS study, blood was drawn for plasma lithium determination and the MR studies were performed as described in the methods. Brain lithium in these 10 patients varied from 0.52 to 0.87 mEq/L (mean = 0.58 mEq/L; SD = 0.17 mEq/L). Brain-to-serum lithium ratios varied from 0.50 to 0.97 mEq/L (mean = 0.77 mEq/L; SD = 0.14 mEq/L). Figure 6 shows the plasma lithium concentrations of these individuals with respect to their daily oral lithium carbonate dosage. As expected, a high correlation ( $r^2 = 0.807$ ) between these variables was found. However, a much poorer correlation ( $r^2 = 0.314$ ) was demonstrated when the brain lithium concentration was compared with the daily dosage. These data are shown in Figure 7. A comparison of serum and brain lithium concentrations in all 10 subjects is displayed on the bar graph of Figure 8. Inspection of this graph reveals a substantial variation in brain-to-serum lithium ratios in different individuals.

TABLE 1: Human in vivo lithium MRS reproducibility<sup>a</sup>

Subject	Scan	Time after First scan	Brain Volume	Brain [Li]	Brain-to-Serum Li Ratio
A	1	NA	846	0.7	0.82
A	2	1.5 h	861	0.68	0.79
B	1	NA	849	0.45	0.83
B	2	1.5 h	824	0.44	0.81
C	1	NA	757	0.89	0.82
C	2	6 mo	1097	0.87	0.88

<sup>a</sup> Three subjects on chronic oral lithium carbonate therapy were each scanned at two different times. Subjects A and B were scanned on the same day, approximately 1.5 hours after they underwent their first scan. Subject C had two studies that were separated by 6 months. The brain volume column refers to the amount of brain sampled during the MRS study and was determined by morphometric analysis of MR images of this brain volume. Brain lithium was determined by MRS, and serum lithium was determined by atomic absorption spectroscopy. NA, not applicable.

## Discussion

Lithium is the drug of choice for the long-term maintenance treatment of bipolar disorder. Many

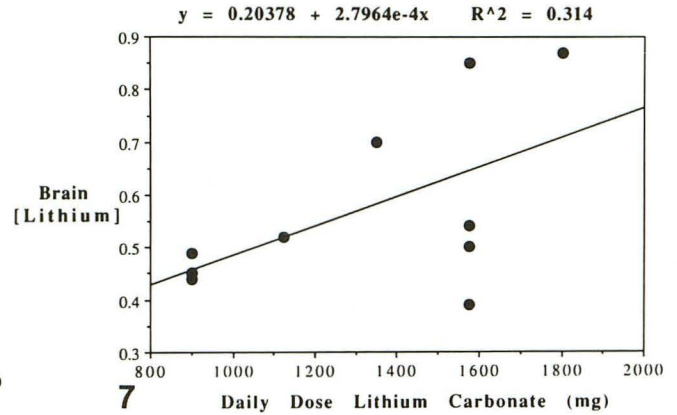
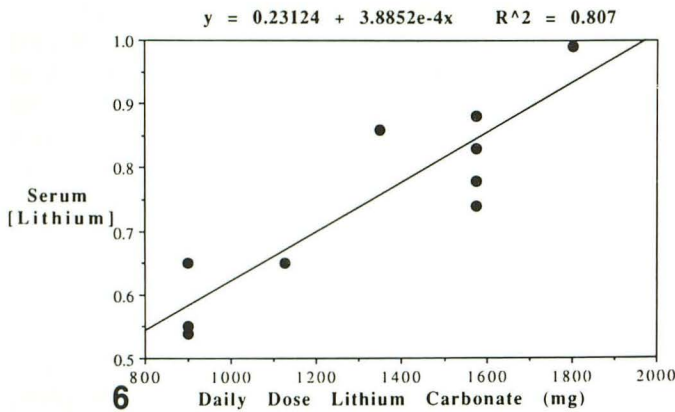


Fig. 6. Daily lithium dose versus serum lithium in 10 patients.

This graph depicts the serum lithium concentration in 10 patients with respect to their daily lithium carbonate oral dose. The serum lithium was determined by atomic absorption spectroscopy.

Fig. 7. Daily lithium dose versus brain lithium in 10 patients.

The brain lithium concentration in the same 10 patients is compared with their daily lithium carbonate dose in this graph. The brain lithium concentration was determined by MRS by the method described in this article.

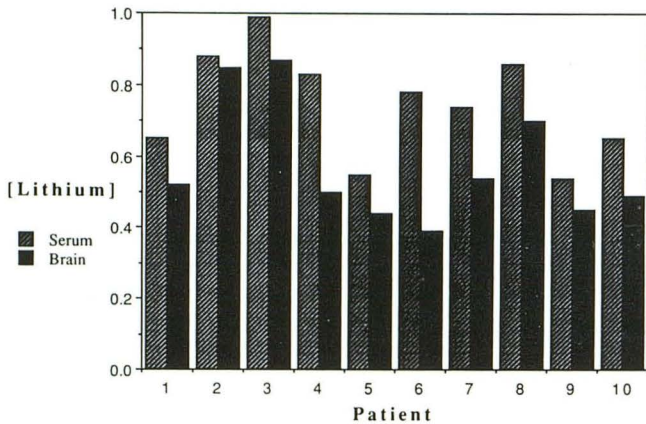


Fig. 8. A comparison of brain lithium and serum lithium concentrations in 10 patients.

The brain and serum lithium concentrations for 10 patients depicted on this bar graph were determined by MRS and atomic absorption spectroscopy, respectively.

controlled studies have demonstrated that lithium is significantly superior to placebo in preventing both manic and depressive episodes (7–10). Although observations suggest a relationship between serum lithium levels and recurrence of affective illness, the relationship remains unclear. A therapeutic range has been established for serum lithium levels. Despite documented compliance, 30% to 50% of patients maintained on therapeutic levels relapse each year (10–12). A fuller understanding of the uneven efficacy of lithium would be likely to result from accurate measures of its concentration within the target organ, the brain. Lithium toxicity is another area of substantial clinical importance in which serum levels have at times proved to be an unreliable

guide (13). The role of differential tissue accumulation in lithium toxicity has not been explored. <sup>7</sup>Li MRS allows for the direct measurement of lithium in the human brain and thus may be useful for the study of these and other clinical issues. However, its utility as a pharmacologic tool requires that it be highly reliable.

The method described in this article to quantify brain lithium concentrations meets the criteria for high reliability. It overcomes the barriers that hinder quantification by in vivo MRS in the following ways.

(a) *Low signal-to-noise ratios due to low ion concentrations are overcome by sampling a large volume, ~1000 mL, of brain tissue.* The ultimate determinant of the precision of any measurement is the signal-to-noise ratio of that measurement. Poor signal-to-noise ratios plague all in vivo MRS experiments because of the low inherent sensitivity of nuclei other than protons and the low tissue concentrations of those spins. Most MR spectroscopists enhance their signal-to-noise ratios by averaging a large number of transients; this is made possible by rapid pulsing. We have undertaken the approach of Bottomley and Hardy (3), who readily obtained high signal-to-noise ratios in <sup>31</sup>P MR spectra of human brains using a 1D-ISIS method to measure from a 3-cm brain section. We measure from a 6-cm section, which results in an excellent signal-to-noise ratio (see Fig. 5). The major disadvantage of this approach is that we are unable to localize lithium within individual brain structures.

(b) *Uncertain T1 effects are eliminated by a long TR (25 seconds).* Few investigators who use



in vivo MRS allow the  $5 \times T_1$  period between pulses that is necessary to ensure full spin relaxation. The resultant disadvantage is that partial saturation effects occur that may not be properly corrected because of the uncertainty of the  $T_1$  values of the sampled spins. We have measured the  $T_1$  of lithium in the brain of two patients and found the average to be 4.2 seconds. This correlates well with the results from Kushnir et al (7), who reported a human brain lithium  $T_1$  of  $3.4 \pm 0.5$  seconds at 2 T. It is also in good agreement with the value measured in puppy brain at 2.1 T (14). By waiting 25 seconds between pulses, our method completely eliminates uncertainties due to partial saturation effects.

(c) *T2 effects are minimized by collecting the FID immediately after excitation.* The finite length of the excitation pulses will result in a slight loss of signal due to  $T_2$  decay. Although we have not directly measured the  $T_2$  of lithium in the human brain, it has been reported to be 80 milliseconds or more in the puppy brain (14). The phantom  $T_2$  was on the order of 100 milliseconds. Thus, the difference in relative signal loss due to finite pulse widths that exists between the lithium within the brain and the phantom is negligible.

(d) *Radio frequency transmission is made homogeneous by the use of adiabatic 90-degree and 180-degree pulses.* Radio frequency coils are imperfect. The practical result of such imperfections is that it is not possible with commonly used hard and soft pulses to excite all of the spins uniformly within the sample. Technically, this is known as  $B_1$  inhomogeneity. Different coils have different  $B_1$  inhomogeneities. Surface coils generally have the worst  $B_1$  inhomogeneity, whereas "bird-cage" coils are generally best in this regard. The effect of nonuniform and generally unknown spin nutations is the addition of a source of systematic error that cannot easily be corrected by postprocessing algorithms. We overcome this problem by the use of adiabatic pulses, which are capable of producing a uniform degree of spin nutation over a wide range of  $B_1$  values (5, 6). An additional practical advantage is that once the adiabatic condition has been achieved at a particular radio frequency power level, increases in the radio frequency power do not alter spin nutation.

(e) *Errors in the calculation of sampled volumes are minimized by the use of computerized morphometric analysis.* Our goal is the determination of the amount of lithium within a well-defined volume of brain. The denominator in the calculation, brain volume, must be accurate.

However, the brain is a complex structure and presents difficulties for the accurate determination of its volume. Traditional methods are unsatisfactory. We overcome this complexity by using a computer-based tool that allows the accurate measurement of brain structures. This tool allows the avoidance of simple and common confounders such as variable ventricular size and sulcal widths.

(f) *Radio frequency reception inhomogeneities are corrected by the use of a mathematical model based on empirically derived data.* The imperfections of radio frequency coils result in differential sensitivity to signals from spins, depending on the position of those spins within the coil. There are several potential solutions to this problem. One is to use a design that is more homogeneous, a bird-cage coil, for example. Within the center of such a coil, both excitation and reception of signal are quite homogeneous. However, to implement the method properly, the diameter of the coil should be made substantially greater than the diameter of the head; this will result in a decrease in the signal-to-noise ratio. We have opted to use the simple Alderman-Grant coil design with a small diameter and then to measure and correct for the receiver inhomogeneity of the coil.

Error analysis predicts a precision of  $\sim 5\%$  and an accuracy of  $\sim 7\%$  in someone with a brain lithium concentration of around 1 mEq/L. As described in the results, the empirical data from both phantoms and patients resulted in a precision that was better than predicted. Indeed, the reproducibility of this method approaches that of clinical measurements of lithium serum concentrations, indicating that it is sufficiently reliable for rigorous pharmacologic studies.

$^7\text{Li}$  has both a high NMR sensitivity (0.293 relative to proton) and a high natural abundance (92.6%) (15). The feasibility of detecting and imaging the distribution of the ion was initially demonstrated in small animals (14, 16), followed by the measurements of a normal volunteer who had been administered both single and multiple doses of lithium carbonate (17). In these initial reports, a surface coil was used to detect signal. We achieved quantification after correction for  $T_1$  effects by using a double-tuned ( $^1\text{H}/^7\text{Li}$ ) coil and comparing the tissue signal with that of an agarose phantom that contained lithium (18). These results suggested that serum lithium levels rose much faster than tissue levels after both single and multiple doses.

Komoroski et al (19) used a single-tuned surface coil technique to report results from a patient diagnosed as having schizoaffective disorder. This patient was studied six separate times over a 7-month period and had a brain-to-serum lithium ratio of  $0.60 \pm 0.13$ , with absolute brain lithium levels ranging from 0.45 to 0.84 mEq/L. Some of this large variation correlated with changes in serum level ( $r = 0.67$ ). Gyulai et al (20) used the dual-tuned surface coil method to measure steady-state brain and muscle lithium levels in nine patients with bipolar affective disorder in remission. They reported an average brain-to-serum lithium ratio of  $0.47 \pm 0.12$  and an average muscle-to-serum lithium ratio of  $0.66 \pm 0.20$ . More recently, Kushnir et al (7) have reported brain lithium levels from three patients with bipolar disorder by also using the method of Renshaw and Wicklund (17). They calculated an average brain-to-serum lithium ratio of  $0.73 \pm 0.06$ . The major technical problems that limited the earlier in vivo studies were, first, a lack of spatial localization other than the use of a surface coil, and second, errors that were introduced by the collection of spectra from spins that were not fully relaxed. No in-depth analysis of likely sources of error or attempts at estimating the precision and accuracy of these surface coil-based measurements were presented. Our own method was developed in response to these and other technical limitations. Despite the different methodologies used, there is an overall agreement, at least in the order of magnitude of lithium concentrations within the brains of patients taking lithium.

The preliminary clinical study on 10 bipolar patients reported here produced intriguing results. A relatively poor correlation ( $r^2 = 0.314$ ) between daily dosage and brain lithium levels was found. Individuals with similar dosages and serum lithium levels were found to differ substantially in brain lithium levels. For example, it can be seen in Figure 8 that patients 2 and 6, who were both on 1575 mg of lithium carbonate per day, have similar serum levels, 0.88 and 0.78 mEq/L, respectively. However, the brain lithium level of patient 2 was found to be more than two times higher (0.85 mEq/L) than that of patient 6 (0.39 mEq/L). Such individual variation in brain lithium levels may help to explain the differences in response to lithium therapy. Differing tissue levels may also provide insights into the source of lithium toxicity in patients who have "therapeutic" lithium serum concentrations.

The significance of an average brain lithium level is confounded by the fact that regional variation in the distribution of brain lithium has been reported. In rats, the chronic administration of lithium leads to relatively high levels in the hypothalamus and striatum, as well as a higher level in white than in gray matter (21, 22). In monkeys, the highest levels of lithium were found in the caudate, thalamus, fornix, and cingulum; the lowest levels were found in the cerebellum, cerebral cortex, and spinal cord (23).

A small number of studies reporting postmortem brain levels in people have been published. Regional brain levels of lithium varied from 0.19 mEq/kg in the temporal cortex to 1.49 mEq/kg in the cingulate gyrus of an individual who had been taking lithium chronically before his suicide (23). Other structures that accumulated lithium included the caudate nucleus, the hypothalamus, and the hippocampus. The whole-blood lithium level in this patient was 0.86 mEq/L; a serum level was not determined. In two patients who died of medical illnesses 3 and 4 days after starting lithium therapy, regional brain lithium levels varied from 60% to 80% of the corresponding serum levels (24). In these patients, the pons had the highest regional lithium level and the cerebral gray matter had the lowest, with the cerebral white matter at an intermediate level.

Taken together, these in vitro results show two general trends. First, periventricular structures tend to have higher lithium levels than more peripheral brain regions. This supports the suggestion that the choroid plexus may be the major source of lithium influx to the central nervous system (25). Second, white matter may accumulate lithium in higher concentrations than gray matter, possibly because of the higher density of voltage-sensitive  $\text{Na}^+$  channels on axons. This could lead to intraneuronal lithium levels that vary as a function of activity; the intraneuronal lithium concentration in squid giant axon is directly proportional to the number of axon potentials it conducts in vitro (26). This would provide a mechanism whereby brain lithium levels might vary as a function of affective state and associated changes in cerebral metabolism.

In conclusion, a method to measure noninvasively the brain concentration of lithium in people by MRS has been presented. The method has been found to be highly reliable. Initial clinical studies have revealed substantial differences in the brain lithium levels of individuals with similar serum levels. Further exploration of discrepancies

between serum and brain lithium levels may help to clarify the variable efficacy of this ion in the treatment of bipolar illness. The major disadvantage of the method is that regional variations in the lithium concentration cannot be determined. Despite this disadvantage, the high reliability of the method indicates that it may become a valuable tool in the study of the neuropsychopharmacology of lithium treatment in bipolar disease.

## Acknowledgments

We thank Dr. Justin Pearlman for the use of his software program used for image morphometry. We gratefully acknowledge the help of Joanne Fordham, Susan Robinson, and Cindy Carr in the preparation of the manuscript.

## References

1. Alderman D, Grant D. An efficient decoupler coil design which reduces heating in conductive samples in superconducting spectrometers. *J Magn Reson* 1979;36:447-451
2. Bottomley P, Foster T, Darrow R. Depth resolved surface coil spectroscopy (DRESS) for in vivo  $^1\text{H}$ ,  $^{31}\text{P}$  and  $^{13}\text{C}$  NMR. *J Magn Reson* 1984;59:338-342
3. Bottomley P, Hardy C. Rapid, reliable in vivo assays of human phosphate metabolites by nuclear magnetic resonance. *Clin Chem* 1989;35:392-395
4. Ordidge R, Connelly A, Lohman J. Image-selected in vivo spectroscopy (ISIS) a new technique for spatially selective NMR spectroscopy. *J Magn Reson* 1986;66:283-294
5. Silver M, Joseph R, Chen C, Sank V, Hoult D. Selective population inversion in NMR. *Nature* 1984;310:681-683
6. Staewen R, Johnson A, Ross B, Parrish T, Merkle H, Garwood M. 3-D FLASH imaging using a single surface coil and a new adiabatic pulse, BIR-4. *Invest Radiol* 1990;25:559-567
7. Kushnir T, Itzhak Y, Valevski A. T1 relaxation times and concentrations of lithium-7 in the brain of patients receiving lithium therapy. *Soc Magn Reson Med* 1991, 1063.
8. Bastrup P, Poulsen J, Schou M, Thomsen K, Amdisen A. Prophylactic lithium: double blind discontinuation in manic-depressive and recurrent-depressive disorders. *Lancet* 1970;326-330
9. Coppen A, Noguera R, Bailey J, et al. Prophylactic lithium in affective disorders. *Lancet* 1971;2:275-279
10. Prien R, Klett C, Caffey E. Lithium carbonate and imipramine in prevention of affective episodes. *Arch Gen Psychiatry* 1973;29:420-425
11. Dunner D, Fieve R. Clinical factors in lithium carbonate prophylaxis failure. *Arch Gen Psychiatry* 1974;30:229-233
12. Goodwin F, Jamison K. Maintenance medical treatment in manic-depressive illness. New York: Oxford University Press, 1990
13. Jefferson J. Lithium poisoning. *Emerg Care Q* 1991;7:18-28
14. Renshaw P, Haselgrove J, Bolinger L, Chance B, Leigh J. Relaxation and imaging of lithium in vivo. *Magn Reson Imaging* 1986;4:193-199
15. Wehrli F. Temperature-dependent spin-lattice relaxation of  $^7\text{Li}$  in aqueous lithium chloride. *J Magn Reson* 1976;23:527-532
16. Renshaw P, Haselgrove J, Leigh I, Chance B. In vivo nuclear magnetic resonance imaging of lithium. *Magn Reson Med* 1985;2:512-516
17. Renshaw P, Wicklund S. In vivo measurement of lithium in humans by nuclear magnetic resonance spectroscopy. *Biol Psychiatry* 1988;23:465-475
18. Thulborn K, Ackerman J. Absolute molar concentration by NMR in inhomogeneous B1. A scheme for analysis of in vivo metabolites. *J Magn Reson* 1983;55:357
19. Komoroski R, Newton J, Walker E, et al. In vivo NMR spectroscopy of lithium-7 in humans. *Magn Reson Med* 1990;15:347-356
20. Gyulai L, Wicklund S, Greenstein R, et al. Measurement of tissue lithium concentration by lithium magnetic resonance spectroscopy in patients with bipolar disorder. *Biol Psychiatry* 1991;29:1161-1170
21. Edelfors S. Distribution of sodium, potassium, and lithium in the brain of lithium-treated rats. *Acta Pharmacol Toxicol* 1975;37:387-392
22. Ghoshdastidar D, Dutta R, Poddar M. In vivo distribution of lithium in plasma and brain. *Indian Exp Biol* 1989;27:950-954
23. Spirtes M. Lithium levels in monkey and human brain after chronic, therapeutic, oral dosage. *Pharmacol Biochem Behav* 1976;5:143-147
24. Francis R, Traill M. Lithium distribution in the brains of two manic patients. *Lancet* 1970;2:523-524
25. Ehrlich B, Diamond J. Lithium, membranes, and manic depressive illness. *J Membr Biol* 1980;52:187-200
26. Ehrlich B, Russell J. Lithium transport across squid axon membrane. *Brain Res* 1984;311:141-143